Supplementary material

S1. Effect of grid discretization

In a realistic solid-liquid interface, the transition between the ordered solid and the disordered liquid takes place gradually over a distance of several inter-atomic spacings. Henceforth, it is impractical and computationally challenging for us to perform phase-field simulations in the realistic length scale. Through the advantage of thin interface limit, the simulations via the phase-field modeling approach are generally performed at an upscaled length scale, and thereby replicate the atomistic scale interfacial features. In this regard, in the present section, we study the role of grid discretization on our numerical simulations, whereby we simulate a four-fold anisotropic dendrite in a supersaturated melt of composition $\Delta = 0.5$ and with an anisotropic strength $\delta_{\alpha\beta} = 0.02$. In order to investigate the effect of discretization errors, we systematically decrease the ratio $\dfrac{\Delta x}{\epsilon}$ and then evaluate the steady state tip velocity V_{tip} for all the simulations. Here, Fig. S1 depicts the tip velocity as a function of the ratio $\dfrac{\Delta x}{\epsilon}$, where we notice that the chosen grid spacing has little influence on the growth rate and primarily does not change its value by more than 3%. For the present study, the chosen discretization spacing $\Delta x = 1.0$ and interface width $\epsilon = 4.0$, and therefore the ratio $\dfrac{\Delta x}{\epsilon} = 0.25$ accounts very well for all our two-dimensional phase-field simulations.

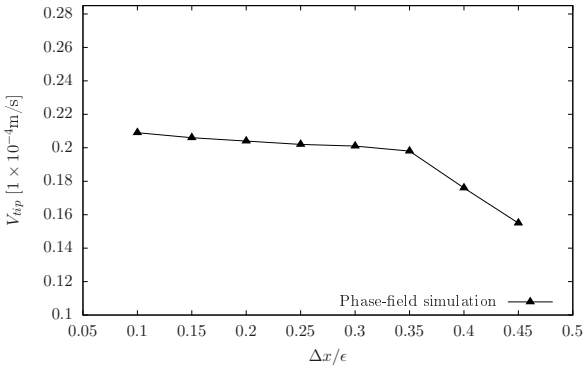

Figure S1.: Tip velocity as a function of the ratio $\dfrac{\Delta x}{\epsilon}$. For all our two-dimensional simulation, we choose $\dfrac{\Delta x}{\epsilon} = 0.25$, and thereby the discretization errors have no influence on our numerical results.

S2. Effect of lattice anisotropy

In continuation with our study on lattice anisotropy, the procedure from the manuscript is repeated for stronger anisotropic strengths $\delta_{\alpha\beta}$ and a direct comparison is shown in Fig. S2, where, for stronger $\delta_{\alpha\beta}$, an excellent agreement between the phase-field simulated equilibrium shape and the sharp-interface crystal shape is achieved.

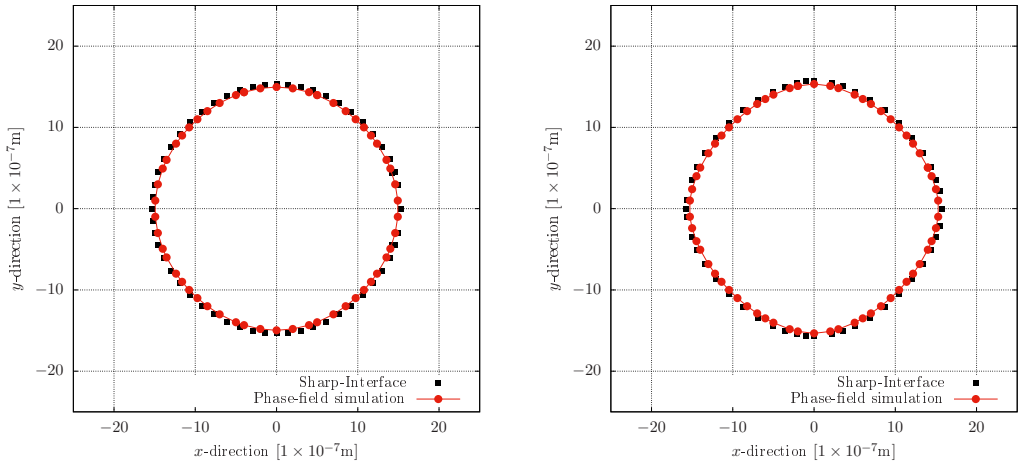

(a) $\delta_{\alpha\beta} = 0.01$ (b) $\delta_{\alpha\beta} = 0.03$

Figure S2.: (a)-(b) For an equilibrium shape with radius $R_0 = 15$, the effect of lattice anisotropy at two different anisotropic strengths. A direct comparison shows an excellent agreement with the sharp interface theory for both cases. Here, the obtained effective anisotropies are $\delta^e_{\alpha\beta} = 0.0096$ for $\delta_{\alpha\beta} = 0.01$, and, $\delta^e_{\alpha\beta} = 0.028$ for $\delta_{\alpha\beta} = 0.03$ respectively.

In addition, for various two-dimensional spherical crystal radii r_0, the role of lattice anisotropy is also investigated. For various seed radii, we notice from Figs. S3, S4 and Fig. S5 that the effective anisotropy depends weakly on the selected r_0. Lastly, it is important to note that for all cases, the effective anisotropy $\delta^e_{\alpha\beta}$ varies less than 5% of the imposed value, and in turn represents the accuracy in our phase-field results.

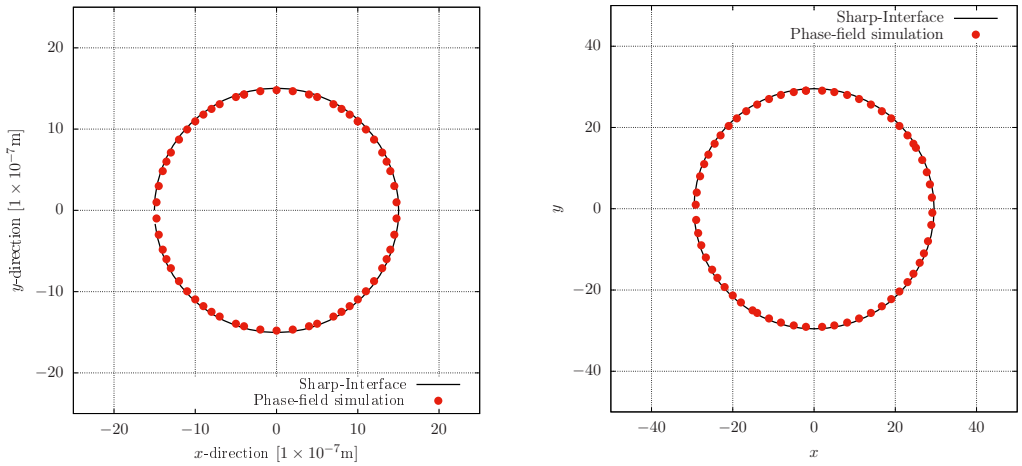

(a) $r_0 = 15$ (b) $r_0 = 30$

Figure S3.: (a)-(b) For an energetically isotropic interface $\delta_{\alpha\beta} = 0.0$, the effect of lattice anisotropy on equilibrium crystals with two different crystal radii. A direct comparison shows an excellent agreement with the sharp interface theory for both cases. Here, the obtained effective anisotropies are $\delta^e_{\alpha\beta} = 0.0005$, $\delta^e_{\alpha\beta} = 0.00015$ for $r_0 = 15$ and $r_0 = 30$, respectively.

S3. Tip splitting phenomenon

In addition to the tip splitting phenomenon discussed in the manuscript for $\alpha = 0.02$, in this section, we further validate the tip splitting phenomenon via modifying the interfacial curvature of the initial interface profile, i.e., modifying the parameter α in the $f(x) = -\alpha(x-h)^2 + p$. In Figs. S6 and S7, we observe that for two different α, the tip splitting phenomenon occurs in accordance with the analytical criterion and in the same regions as given by Eq. (13) in the manuscript. The tips evolve in the crest regions while the inhibited part of the interface is within the trough region. Moreover, as the interfacial

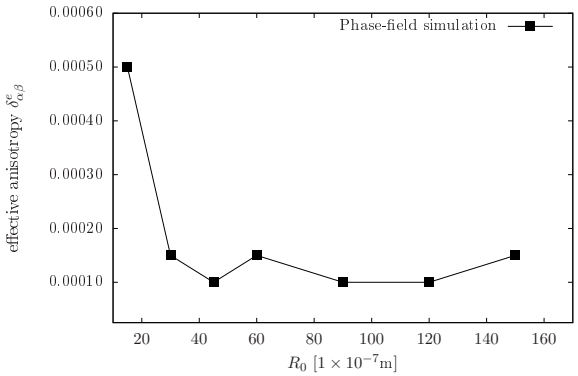

Figure S4.: Effective anisotropy induced due to the underlying lattice as a function of the seed radius r_0 at an imposed interfacial strength $\delta_{\alpha\beta} = 0.0$ and $\dfrac{\Delta x}{\epsilon} = 0.25$.

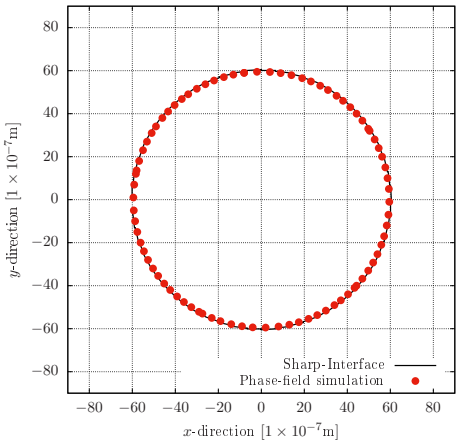

Figure S5.: Effect of lattice anisotropy on an equilibrium crystal with radius $r_0 = 60$, where an excellent agreement with the sharp interface theory is observed. Here, the obtained effective anisotropy $\delta^e_{\alpha\beta} = 0.00015$.

curvature increases from $\alpha = 0.02$ to $\alpha = 0.04$, we notice that the splitting is more profound and amplified during solidification.

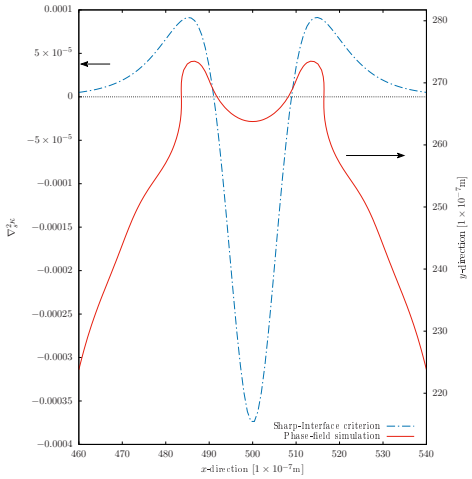

Figure S6.: Tip splitting phenomenon in complete agreement with the analytical criterion for $\alpha = 0.025$

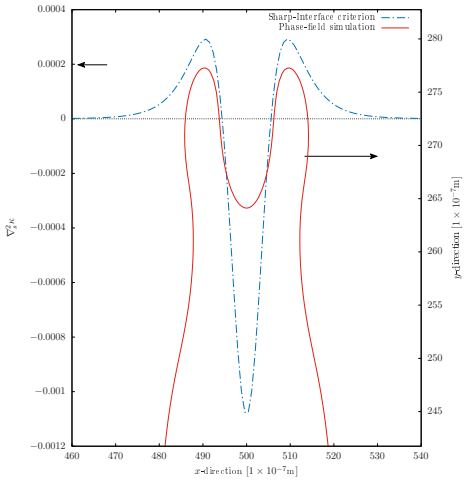

Figure S7.: Tip splitting phenomenon in complete agreement with the analytical criterion for $\alpha = 0.04$